

Observations of Lubricated Rolling Contact Fatigue on Silicon Nitride Rods

M. Hadfield & T. A. Stolarski

Brunel University, Department of Mechanical Engineering, Uxbridge, Middlesex UB8 3PH, UK

(Received 5 April 1994; accepted 6 September 1994)

Abstract: Lubricated rolling fatigue tests on silicon nitride rods are discussed. Fully densified micro-porous and porous silicon nitride rods are tested using a disc-on-rod method. Failure modes and surface fatigue spalls are examined using scanning electron and light microscopy. The degree of porosity in silicon nitride and its influence on manufacture and quality is discussed.

1 INTRODUCTION

The use of ceramics for rolling contact element bearing applications has become a reality for some specialist applications. Three rolling element bearing applications where ceramics are considered as a replacement for traditional steels are gas-turbine engines, grinding machine tools and milling machine tools. The two principal reasons why ceramics are considered for these applications are that low density reduces centrifugal force effects (high speed machinery such as gas turbine engines and grinding applications) and a moderate increase in elastic modulus increases the dynamic stiffness (milling applications).

In the case of gas turbine engines, the thermal efficiency increases as shaft speed increases but centrifugal loads also increase. The contact stress acting on the outer race of the rolling element shaft bearings can cause premature failure because of the increased rotational speed. One option to reduce the contact stress is to replace the rolling element balls or rollers within shaft bearings with lower density ceramics. Silicon nitride is usually chosen for this type of application due to its overall suitability of physical properties, i.e. low density and moderate elasticity modulus, with good toughness and fatigue life.

Preliminary rolling contact tests by Scott and Blackwell¹ and Scott *et al.*² on reaction bonded silicon nitride gave poor results compared to bearing steel. A factor thought to influence the poor

rolling contact fatigue resistance was micro-structure porosity. Since then, hot isostatic pressed (HIP) pre-sintered silicon nitride preforms, and enhanced additive technology have enabled a fully densified material to be produced. This material can achieve a fully densified, high quality micro-structure with suitable mechanical properties that is challenging traditional bearing steels in rolling contact applications. Substantial rolling contact testing is still required to enable the material to reach its potential in this application.

This present study reviews previous experimental studies of rolling contact fatigue of silicon nitride rods. Present tests are conducted on fully densified, micro-porous and porous silicon nitride. Results are presented and surfaces are examined by scanning electron and light microscopy.

1.1 Some previous experimental studies

Comparative rolling fatigue studies of hot-pressed silicon nitride, hot isostatically pressed silicon nitride, sialon and M50 bearing steel were reported by Lucek.³ A rod type fatigue testing machine in which three 12.7 mm diameter steel balls orbit a rotating 9.53 mm diameter cylindrical test specimen was used. Results showed that the predominant fatigue failure mechanism of silicon nitride involves the slow growth of circumferential cracks from the edges of the contact path driven by tensile stresses. Spalling occurred when material in the compressive zone was insufficiently supported.

Rolling contact fatigue data⁴ of good quality silicon nitride produced by the HIP technique was compared with poor quality silicon nitride and M50 steel. This was conducted to compare silicon nitride with a traditional bearing steel which is used in gas turbine aircraft engine applications. It is important to study the effects of ceramic material quality on its rolling contact fatigue performance, poor quality silicon nitride being defined as material of high porosity and containing inclusions. These materials were tested using a disc-on-rod machine. The results showed that under certain conditions good quality silicon nitride could outperform M50 steel. The surface fatigue mode of the silicon nitride for all cases was spalling. Edge cracks as found by Lucek³ were not reported, confirming that this may not be the only failure mechanism.

Earlier work using the disc-on-rod machine was done by Lucek and Cowley⁵ with a hot-pressed silicon nitride test specimen. All failures were of a spalling, non-catastrophic nature and test loads varied from 4.1 to 5.5 GPa. Reduced fatigue life was caused by cone cracks found on the ceramic surfaces. Surface quality was studied as a function of fatigue life, in particular, the method of specimen finishing. It was found that test specimen finishing by different honing and lapping techniques influenced rolling contact fatigue results. The fact that finishing techniques were influential on test results is not surprising. The shape of asperities varies with finishing technique and silicon nitride materials may be sensitive to this parameter.

Baumgartner⁶ studied the rolling contact fatigue resistance of hot-pressed silicon nitride using the disc-on-rod machine. At these conditions and under various loads the silicon nitride could outperform M50 steel. A spalling, non-catastrophic failure mechanism was again reported.

2 TEST CONDITIONS FOR PRESENT STUDIES

2.1 The disc-on-rod machine

The disc-on-rod machine (Fig. 1) was adopted for the rolling contact fatigue tests. Test rods of 9.53 mm diameter were clamped to the motor drive spindle. Rod eccentricity was checked by a dial test indicator clamped to the machine. Two 200 mm diameter discs with end radius ground to 12.7 mm diameter were rested on the test rod. A force of 2.9 kN was then applied to the contact area by a turnbuckle and measured with a calibrated load cell.

The lubricant was dripped onto the contact

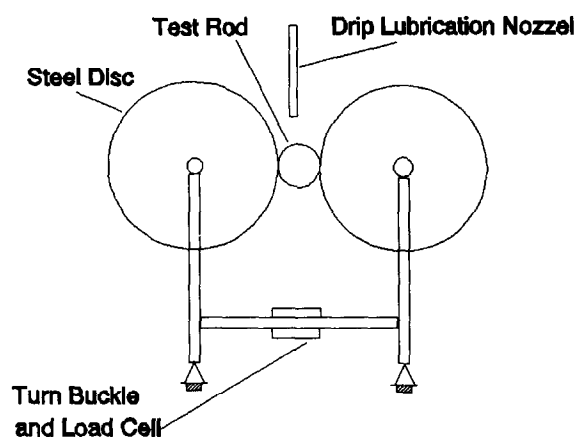


Fig. 1. Schematic diagram of the disc-on-rod machine.

area, the rod driven by an electric motor at 12,500 rpm. This rotation turns the contacting steel discs. Slip between the steel discs and ceramic test rod was 4.6 % and measured by a stroboscope. Disc and rod alignment was adjusted after viewing the lubricant spray from the contact ellipse edges. Testing was stopped automatically when excessive vibration was measured at a set sensitivity.

Table 1 shows the standard test parameters and contact conditions. The maximum compressive contact stress is 5.4 GPa which is calculated using Hertz theory.⁷ When a steel rod is used, the contact stress reduces to 4.8 GPa under the same force and this reflects the difference of silicon nitride elastic modulus. The lambda ratio⁸ is found by calculating the oil film thickness using a dimensional analysis technique and comparing it with the surface roughness. A lambda ratio of 1.6 is within the operating region for most industrial rolling element bearing applications and means that some asperity contact will occur during tests. Rolling contact fatigue resistance is reduced under these conditions compared with tests at lambda values above three.

2.2 Materials tested

Material quality was monitored for all test materials to identify possible failure causes and to insure test consistency. A sample rod from each test batch was sectioned, polished and visually ana-

Table 1. Standard test parameters and contact conditions

Maximum compressive stress (GPa)	4.8 (steel rod) 5.4 (ceramic rod)
Surface roughness (Ra, μm)	0.163 (steel disc) 0.100 (test rod)
Rod speed (rpm)	12,500
Lambda ratio	1.6

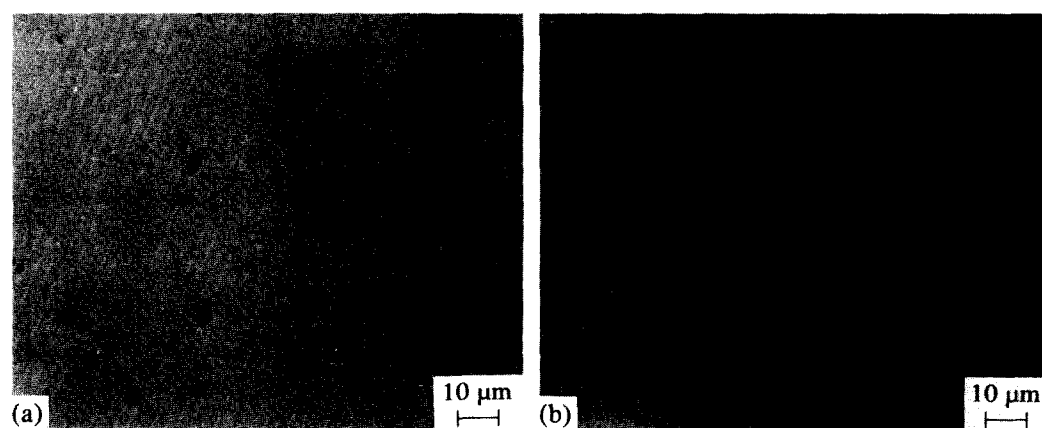


Fig. 2. Material section analysis using an optical microscope ($\times 575$). (a) Typical microstructure, (b) worst feature.

lyzed using an optical microscope. Figure 2 shows a typical section of a silicon nitride containing high porosity levels. The worst area of porosity was approximately $10\ \mu\text{m}$ in length, this represents poor quality silicon nitride material. Fully densified test material quality contains no porosity with fine phases within the microstructure resulting from additives.

3 TEST RESULTS

3.1 Fully densified silicon nitride

Fully densified silicon nitride material rod tests are conducted according to Table 1, i.e. steel contacting discs and Exxon 2389 lubricant. Tests were suspended after thirty million cycles to provide adequate screening and to avoid severe wear to the steel discs. The reduction in contact stress exerted on the silicon nitride rod due to steel disc wear is monitored and taken into account.

The material was tested four times and suspended after thirty six million stress cycles. Here, no pitting or spalling damage is observed on the silicon nitride rod. Surface edge cracks were not visible after surface examination and dye-penetration inspection. It was discussed earlier (Section 1) that Lucek³ did find edge cracks on silicon nitride surfaces. It is generally considered that edge cracks are caused by tensile stresses located on the contact surface periphery. The significance of this fact is that the silicon nitride mode of surface fatigue failure is influenced by the test configuration. Typical wear scars extending to a width of 0.91

mm were observed on the silicon nitride rod surface. The scars are expected with a lambda ratio of 1.6 (Table 1). This means asperity contact between the surfaces is probable, which may subsequently cause adhesive wear.

3.2 Micro-porous silicon nitride

The second set of tests considered a standard bearing steel, and silicon nitride with a structure containing micro-porosity. This test shows how well apparently imperfect silicon nitride material can compare to steel under identical applied loads. It is appreciated that at least 20–100 repeated tests are required to statistically verify the results. Table 2 shows the test materials. Figure 3 indicates the time to failure or suspension of these tests.

The bearing steel test rod failed by a conventional contact fatigue spall (Test 5). Wear scars were observed on the material extending to a width of 0.96 mm. Spall depth, width and length (rolling direction) were measured as $66\ \mu\text{m}$, 0.79 mm and 43 mm, respectively. It should be noted that this steel is specified to moderate operating temperatures and thus has better contact fatigue resistance than a typical high temperature steel,

Table 2. Test conditions for micro-porous silicon nitride

Test	Material	Test stop reason	Lubricant
5	Bearing steel	Spall	Exxon 2389
6	Silicon nitride	Spall (disc)	Exxon 2389
7	Silicon nitride	Suspend	Exxon 2389

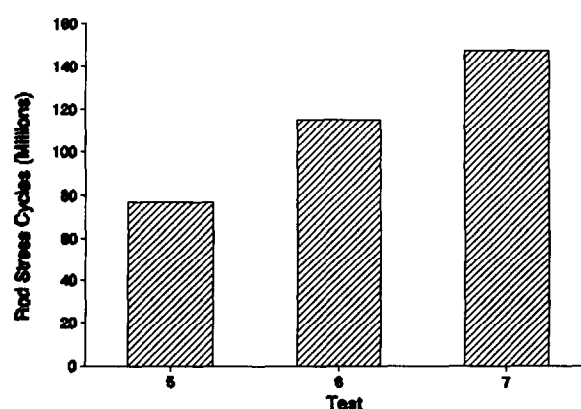


Fig. 3. Ceramic and steel test results.

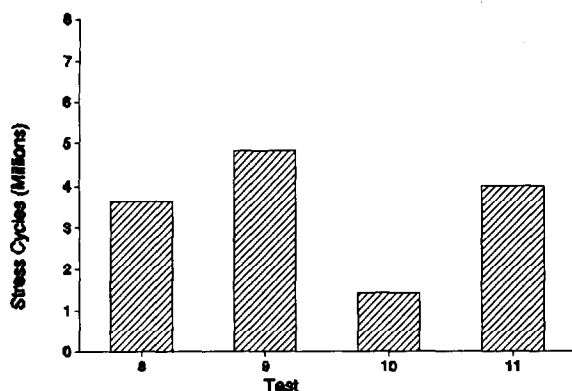


Fig. 4. Substandard ceramic test results.

for example M50. The silicon nitride material may, however, be used at moderate or higher temperatures while maintaining good contact fatigue resistance (Hamburg *et al.*⁹).

Tests on the silicon nitride material that contain a micro-porous structure are shown as 6 and 7 in Table 2 and Fig. 3. These tests were suspended (Test 7) or stopped due to a steel disc spalling (Test 6). Silicon nitride with micro-porosity life extends beyond the steel failure probability band, thus showing that although it is known that porosity is associated with premature contact fatigue failure, the pore density and pore size may have a limiting influence.

3.3 Porous silicon nitride

3.3.1 Standard test

The silicon nitride was designated as poor grade due to its high porosity, large porosity size and inclusions within the structure. The material microstructure is shown as Fig. 2 (Section 2.2), porosity size reaches $10\text{ }\mu\text{m}$ in length. Tests 8–11 examined the material fatigue life under standard conditions described in Section 2.1, and with previously described configurations, i.e. Exxon 2389 lubricant and rod roughness of $0.1\text{ }\mu\text{m}$ Ra. The porous silicon nitride test results are shown in Fig. 4.

It is shown in Fig. 4 that material performance is poor when compared with previous tests of micro-porous silicon nitride and bearing steel. Comparing the present results to the silicon nitride that contains micro-porosity, the fatigue performance is reduced by an order of magnitude. This implies that a limiting degree of porosity size and density within the silicon nitride microstructure may be acceptable. The cost of manufacturing fully dense silicon nitride is high, and specifying quality standards that accept a degree of porosity may be justified both on a technical and economic basis. It is, however, appreciated that it is difficult to control the pore morphology of a porous silicon nitride ceramic.

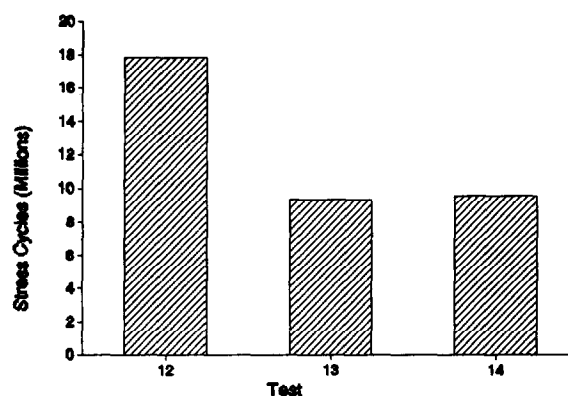


Fig. 5. Substandard ceramic rod test results.

3.3.2 Non-standard test

The rod surface finish was enhanced to $0.05\text{ }\mu\text{m}$ Ra, by diamond polishing in water. Test lubricant was also changed to Talpa 20 base oil, which has greater viscosity ($94.6\text{ cs}^\circ\text{C}$ at 40°C) than the recommended test oil ($12.46\text{ cs}^\circ\text{C}$ at 40°C). These modifications have the effect of increasing the lambda value (oil film thickness and surface roughness function) to above three. This implies little or no asperity contact at the disc/rod interface. Non-standard test results (12–14) are shown in Fig. 5.

The results from Tests 12–14 show that the slight change in tribological conditions affects fatigue life quite dramatically. Here the rod survived at least twice the number of stress cycles. This result shows that although material quality is very important, the material is also extremely sensitive to tribological conditions.

4 FAILURE ANALYSIS AND DISCUSSION

4.1 Influence of porosity

The rolling contact fatigue tests described in Section 3 indicate that the degree of porosity size and density may have a limiting influence on silicon nitride fatigue life. It was established that the silicon nitride which contained micro-porosity could still have a useful fatigue life. The contact path of the micro-porous silicon nitride rod was studied using a dye penetrant technique to provide some explanation to the limiting influence on fatigue life. The silicon nitride rod is treated with a dye penetrant before optical analysis. The rod is then viewed under normal white light and then ultraviolet light. Any cracks, porosity or surface defects are viewed due to the reaction of the penetrant under ultraviolet light.

Microscopic images of Test 7 contact path under white and ultraviolet light are shown in Fig. 6. Figure 6(a) shows the typical contact path of width 0.91 mm , and wear scars are also evident.

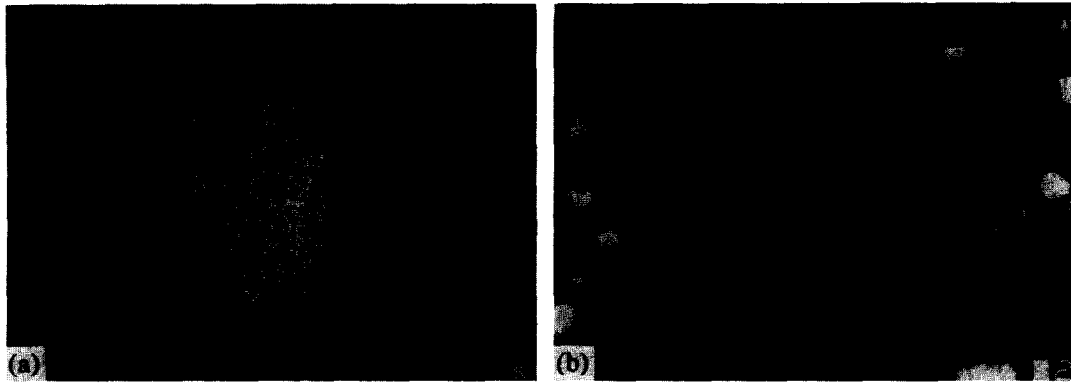


Fig. 6. Optical analysis of the contact path for test seven ($\times 70$). (a) Contact path (rotation \downarrow), (b) contact path (ultraviolet).

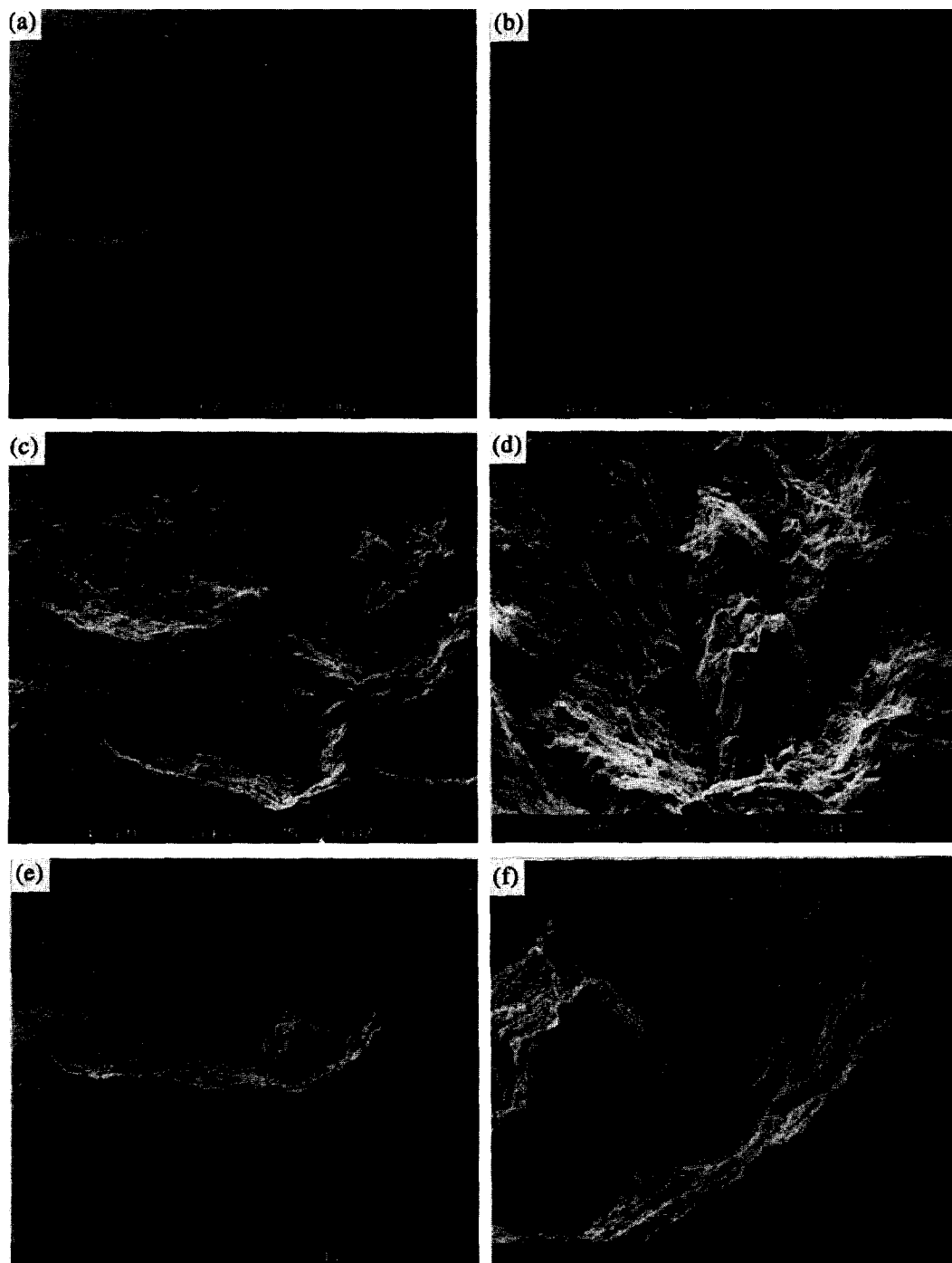


Fig. 7. Micrographs of spall for test eight.

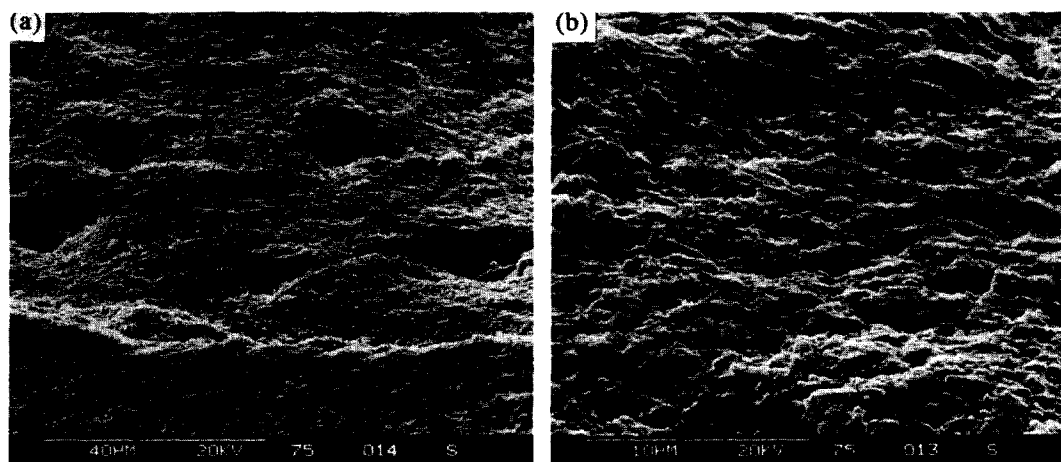


Fig. 8. Micrographs of secondary surface spall (Test 8). (a) Small pores, (b) spall texture.

An identical position under ultraviolet light, Fig. 6(b), shows the contact path edge where the micro-porosity is clearly visible. It should be noted that the pore size is exaggerated due to the illuminance of the dye-penetrant. At the region near the contact path centre, the porosity on the contact path is no longer visible on the surface. It is therefore postulated that limitation of micro-porosity influence is due to surface pores becoming blocked due to specimen wear debris or plastic deformation within the contact area.

4.2 Fatigue spall analysis

Typical rolling contact fatigue spalls are the failure mode on the porous silicon nitride. The failure dimensions shown in Table 3 agree with the stress fields associated with ceramic/steel contacts under the test loads and surface geometry. The comparison of spall dimensions, standard tests (8–11) with non-standard tests (12–14), shows no specific differences resulting from varying test conditions. Surface cracks were not found after extensive surface observations using the dye-penetration method.

Scanning electron microscope observations of

fatigue spalling in Test 8 are shown in Fig. 7. Figure 7(a) shows the failure overview of primary and secondary spalling, and the contact wear path is also evident. The wear path, wear scars and exposed porosity adjacent to the spall are shown in Fig. 7(b). Fatigue surface of the large primary spall is examined in Fig. 7(c) and (d). Surface undulations are visible and exposed debris in the deepest section of the spall can also be seen. The small secondary spall is examined in Fig. 7(e) and (f). Again, debris are located within the trailing spall and undulations are visible.

The secondary spall surface is studied under higher magnification, as shown in Fig. 8. Porosity reaching 20 μm in length is visible on the fracture surface, in Fig. 8(a). Due to material pull-out during fracture, porosity size is greater than twice the maximum pre-test section examination. Striation-like surface texture is observed in Fig. 8(b), where the distance between these markings is between one and two microns. This distance is of similar order to pre-sintered silicon nitride powder.

5 CONCLUDING REMARKS

Silicon nitride tested under standard and non-standard disc-on-rod conditions fails by a non-catastrophic spalling mode. The rolling contact resistance of porous silicon nitride is very sensitive to tribological variations.

Repeated tests are required to evaluate statistical confidence limits on the test results presented. After further tests it may be justified to specify silicon nitride quality standards for rolling element bearing applications that accept a degree of porosity.

The mode of silicon nitride failure using the disc-on-rod machine differs to that found when using the ball-on-disc machine. The influence of edge cracks caused by tensile stress near the con-

Table 3. Spall measurement analysis

Test	Spall width— across contact path (mm)	Spall length— along contact path (mm)	Spall depth (mm)
8	0.67	0.46	0.034
9	0.71	0.46	0.030
10	0.79	0.64	0.082 (0.117 maximum)
11	1.07	0.93	0.040 (0.080 maximum)
12	0.81	0.57	0.100
13	0.53	0.43	0.030
14	0.50	0.64	0.040 (0.150 maximum)

tact region on the rolling contact fatigue mode should be investigated further.

REFERENCES

1. SCOTT, D. & BLACKWELL, J., Hot pressed silicon nitride as a rolling bearing material—a preliminary assessment. *Wear*, **24** (1973) 61–7.
2. SCOTT, D., BLACKWELL, J. & MCCULLAGH, P. J., Silicon nitride as a rolling bearing material—a preliminary assessment. *Wear*, **17** (1971) 73–82.
3. LUCEK, J. W., Rolling wear of silicon nitride bearing materials. *ASME*, 90-GT-165, Presented at the *Gas Turbine and Aero-engine Congress and Exposition*, June 11–14, 1990, Brussels, Belgium.
4. CUNDILL, R. T., Rolling element bearings into the 21st century. *IMechE Seminar Proceedings*, London, November 1990.
5. LUCEK, J. W. & COWLEY, P. E., Investigation of the use of ceramic material in aircraft engine bearings. Dept of Navy, Code AIR-52032A, Washington.
6. BAUMGARTNER, H. R., Ceramics for high-performance applications. *Proc. Second Army Materials Technology Conf.*, Nov. 13–16, Hyannis, Massachusetts, eds Burke, J. J., Gorum, A. E. and Katz, R. N., 1973.
7. JOHNSON, K. L., *Contact Mechanics*. Cambridge University Press, Cambridge, 1985.
8. TALLIAN, T. E., The theory of partial elastohydrodynamic contacts. *Wear*, **21** (1972) 49–101.
9. HAMBURG, G., COWLEY, P. & VALORI, R., Operation of an all-ceramic mainshaft roller bearing in a J-402 gas-turbine engine. *J.ASLE, Lubrication Engineering*, July, 1980.